A mechanism for the downturn in inverse susceptibility in triangle-based frustrated spin systems

2008 J. Phys.: Condens. Matter 20 315202

(http://iopscience.iop.org/0953-8984/20/31/315202)

J. Phys.: Condens. Matter **20** (2008) 315202 (8pp) doi:10.1088/0953-8984/20/31/315202

A mechanism for the downturn in inverse susceptibility in triangle-based frustrated spin systems

M Isoda

Department of Physics, Faculty of Education, Kagawa University, Saiwai-cho 1-1, Takamatsu 760-8522, Japan

E-mail: misoda@ed.kagawa-u.ac.jp

Received 10 December 2007, in final form 4 June 2008
Published 17 July 2008
Online at stacks.iop.org/JPhysCM/20/315202

Abstract

A mechanism for the downturn of inverse magnetic susceptibility below an intermediate temperature, recently observed in many experiments, is proposed as an intrinsic feature of lattices with triangle-based frustrated geometries. The temperature at the bending of the inverse susceptibility curve may be related to the features of other thermodynamic properties; the hump of the specific heat and the emergence of a 1/3 plateau in magnetization under a magnetic field. This fact is derived through a Monte Carlo simulation study of the Ising model on triangular and kagome lattices, and the exact calculation for the single and small-sized triangle clusters, on both the Ising and Heisenberg models. These results may indicate the dominance of $S(S^z) = 1/2$ quantum (classical) trimer formation in the intermediate-energy regime in two-dimensional triangle-based lattices.

1. Introduction

As a feature of frustration, the suppression of long-range ordering or freezing temperature has been well known for various lattice systems, and several recent investigations have focused on exotic low energy properties [1–4]. Recent investigations on newly synthesized systems have aroused interest not only in the low energy regime but also the intermediate energy regime, comparable with the nearest neighbor (nn) exchange interaction.

The intermediate energy phenomenon of interest to us is the sharp upturn of the magnetic susceptibility below intermediate temperatures, commonly found in spin systems with triangle-based frustrated geometry, without any indication of long-range ordering. That is, the inverse susceptibility changes from a high-temperature Curie–Weiss (CW)-like form to a low-temperature Curie-like form. The triangular $NaTiO_2$ [5], kagome $ScCr_{9p}Ga_{12-9p}O_{19}$ (SCGO) [6, 7], $ZnCu_3(OH)_6Cl_2$ [8] and three-dimensional triangle network garnet system $Gd_3Ga_5O_{12}$ [9] are typical examples with regular structures. Several systems with modified structures have also been recognized as showing the feature, for example, volborthite $Cu_3V_2O_7(OH)_2$ (modified kagome system) [10], the bilayer system $Ba_2Sn_2ZnCr_{7p}Ga_{10-7p}O_{22}$ [11], triangular cluster compounds [12, 13] etc.

To the best of our knowledge, this was first detected theoretically as the almost temperature-independent mean-squared magnetization in the low-temperature region in a Monte Carlo (MC) simulation study for the Ising and Heisenberg spins on the triangular lattice by Sano [14]. The mean-squared magnetization gives the susceptibility by dividing by the temperature in the disordered state, then the susceptibility results in the Curie-like temperature dependence. However, the author did not refer to the temperature dependence. A subsequent study might be the phenomenological description for accounting for the susceptibility of SCGO [15] by Schiffer and Daruka [16], where the two separate contributions were assumed to be orphan and correlated spins for two temperature regimes of Curie and CW. As a theoretically controlled approach, high-temperature series expansion [17–19] was carried out for the Heisenberg model in two-dimensional frustrated lattices. However, this approach does not seem to have succeeded in giving sufficient upturn of susceptibility as found in the experimental results. For the kagome system $ZnCu_3(OH)_6Cl_2$, the origin was attributed to the Dzyaloshinski–Moriya interaction [20] or defects due to Zn/Cu exchange [21]. In addition to the bending in the inverse susceptibility, we note the fact that most of these experimental studies reveal a broad

peak of the specific heat near the temperature of bending of susceptibility [9].

The purpose of the present study is to attempt to elucidate a mechanism for the downturn in inverse susceptibility below an intermediate temperature, which has been found experimentally. This seems to be common in antiferromagnetic spin systems with triangle-based lattices. Furthermore, it is important to clarify whether the mechanism brings the broad peak in the specific heat. We carried out an MC simulation study for thermodynamical quantities of the $s = 1/2$ Ising model on frustrated triangular and kagome lattices. An MC study of these quantities has also been carried out in previous studies [22–25]; however, attention has not been paid to the upturn in susceptibility in these studies and, furthermore, the relationship with the behavior of other thermodynamical quantities. The weak system-size dependence of the qualitative features in the temperature dependence of thermodynamical quantities observed in the present MC study has directed us to the exact calculation of quantities for the single triangle cluster and for small-sized ones. This approach is also expected to be supported by the generally believed short correlation lengths in frustrated systems [26]. The magnetization as a function of the magnetic field is also calculated to study the 1/3 plateau found below the temperature characterized by the bending in susceptibility and the hump in the specific heat.

The paper is structured as follows. In section 2, the results of the MC simulation are given for the specific heat, magnetic susceptibility and magnetization under a magnetic field in the spin-1/2 antiferromagnetic Ising model on triangular and kagome lattices. In section 3, these quantities are calculated exactly for a single triangle and small-sized clusters. Section 4 is devoted to discussion and the conclusions.

2. Monte Carlo simulation study

MC simulation was applied for the spin-1/2 antiferromagnetic Ising spin model for triangular and kagome lattices, to investigate the specific heat, magnetic susceptibility and magnetization under a magnetic field. The former two quantities have already been studied by several researchers using the same method [22–24]. However, the calculation is performed again to demonstrate the inverse form of the susceptibility (which was not shown in the previous studies) and to mark the characteristic temperature discussed below. The magnetization process has also been investigated in the Ising and XXZ models, including the Ising limit on triangular [27–30] and kagome lattices [31, 32]. However, these three thermodynamical quantities have not been considered previously with focus on the relationships between them.

We have used the usual Metropolis algorithm with a periodic boundary condition, and MC averages were taken over 10^4 MC steps usually after 10^4 thermalization MC steps. For checking the MC uncertainty, we have made test runs with up to 10^6 steps both for averaging and thermalization steps; however, no remarkable difference was detected to suggest a meaningful effect in the present discussion.

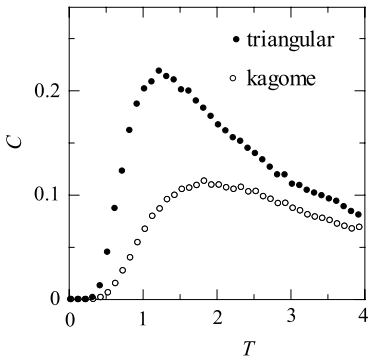

Figure 1. The specific heat per spin, C, as a function of T for triangular (closed circle) and kagome (open circle) lattices composed of $50 \times 50 \times 3$ spins by MC simulation.

The Hamiltonian for the spin-1/2 Ising model is expressed as

$$\tilde{H} = 4H = J \sum_{\langle i,j \rangle} \sigma_i \sigma_j - h \sum_i \sigma_i, \tag{1}$$

where $\sigma_i = 2s_i^z$. s_i^z is the z-component of the ith spin and h is the magnetic field. The summation on $\langle i, j \rangle$ denotes it over the nn sites i and j. The exchange coupling constant is set to unity ($J = 1$) with units of energy hereafter for the antiferromagnetic interaction. H gives the Hamiltonian for the original spin variable $\boldsymbol{s}$ with the usual expression.

The specific heat, magnetization and longitudinal (z-component) uniform magnetic susceptibility per spin are evaluated by the following formulas, respectively:

$$C = \frac{1}{N_0 T^2}[\langle E^2 \rangle - \langle E \rangle^2], \tag{2}$$

$$m = \frac{1}{N_0} \left\langle \left| \sum_i \sigma_i \right| \right\rangle, \tag{3}$$

$$\chi = \frac{1}{N_0 T} \left[\left\langle \left(\sum_i \sigma_i \right)^2 \right\rangle - \left\langle \sum_i \sigma_i \right\rangle^2 \right]. \tag{4}$$

Here, N_0 represents the total number of spins, T is the temperature in units of the Boltzmann constant and E is the internal energy of the system given by the Hamiltonian $\tilde{H}$. The thermal average $\langle A \rangle$ denotes $\langle A \rangle = \mathrm{Tr}(\mathrm{e}^{-\beta \tilde{H}} A)/Z$, where Z is the partition function of the system, Tr stands for the trace operation and $\beta = 1/T$.

The results for the specific heat C and inverse uniform magnetic susceptibility χ^{-1} are shown in figures 1 and 2, respectively, both for the triangular and kagome lattices. These results are obtained for a system size of $L \times L$ unit cells of the triangle at $L = 50$; in other words, the total number of spins $N_0 = L \times L \times 3$. The results of the specific heat are consistent with those in [21, 22], showing a broad hump for both lattices as a remarkable feature. This hump will be discussed in section 3.

The inverse susceptibilities for both lattices show the distinct downturn deviation from the Curie–Weiss-like form at high temperature to the Curie-like one at low temperature, as

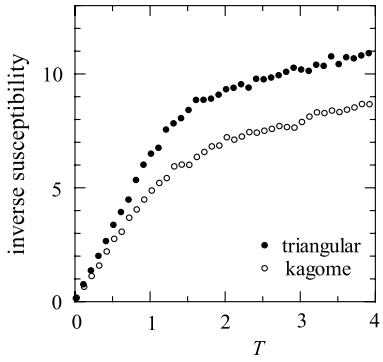

Figure 2. The inverse uniform magnetic susceptibility per spin, χ^{-1}, as a function of T for triangular (closed circle) and kagome (open circle) lattices composed of $50 \times 50 \times 3$ spins by MC simulation.

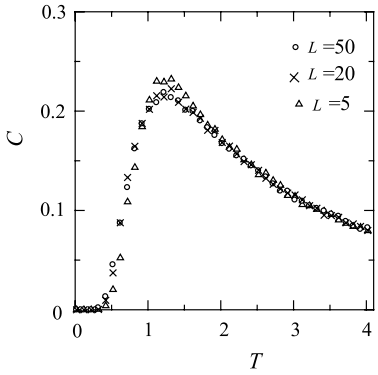

Figure 4. The system-size dependence of the specific heat per spin as a function of T for the triangular lattice. ∘ represents $L = 50$, × represents $L = 20$ and △ represents $L = 5$.

shown in figure 2. This temperature dependence is qualitatively consistent with that of the mean-squared magnetization in [14]. In previous investigations, the downturn deviation has not been recognized and/or properly paid attention to, because the susceptibility itself, not its inverse, was plotted in figures. This feature is one of the two issues of interest in this study and the microscopic interpretation for this will be given in section 3. The temperature corresponding to the bending nearly coincides with the temperature at the top of the hump in the specific heat for each lattice. Then, these temperatures are roughly estimated as characteristic temperatures $T^{\ell}_{\text{triangular}} \sim 1.3$ and $T^{\ell}_{\text{kagome}} \sim 1.6$, in triangular and kagome lattices, respectively. The present lower-temperature Curie-like behavior should be distinguished from that due to magnetic impurities, often found in experimental results at sufficiently low temperatures ($T \ll J$).

The magnetization is also computed as a function of h. The magnetization reveals the well known $1/3$ plateau [27] in both lattices as shown in figure 3. This $1/3$ plateau state is believed to be the up–up–down (uud) state in the three-sublattice structure [28, 32]. In the figure, we recognize that the plateau approximately disappears for temperatures higher than the characteristic temperature $T^{\ell}_{\text{triangular}}$ or T^{ℓ}_{kagome} defined above. At $T = 0$, the magnetization is expected to take $1/3$ of the maximum value(=1) for an infinitesimally weak field and jumps from $1/3$ to the maximum value through the first order transition in the present Ising model, as readily imagined, as a spin flip of the down spin from the uud state. The plateau at low temperature and in a weak field strongly suggests the existence of free spins of one-third the total number of spins in the ground state manifold. The disappearance of the plateau above the characteristic temperatures is discussed, similar to the hump of specific heat, from the energy scheme of clusters given in section 3.

For investigating the system-size effect on three physical quantities, we have calculated the specific heat and the magnetic susceptibility for three system sizes, $L = 50$, 20 and 5. The results indicate that size dependence is not remarkable for both lattices, as shown in figures 4 and 5 only for the triangular lattice. It is amazing that even for the very small size of $L = 5$, no remarkable change is found in comparison with those of the larger sizes.

The characteristic temperatures defined above roughly correspond to the magnitude of the coupling constant J, that is, nearly equal to unity. Thus, the higher-temperature regime is the region where each spin interacts individually under the antiferromagnetic interaction in the mean-field sense, resulting in CW-like susceptibility with a negative Weiss constant, similar to the case of non-frustrated lattices. Otherwise, how should the lower-temperature regime be characterized? Some

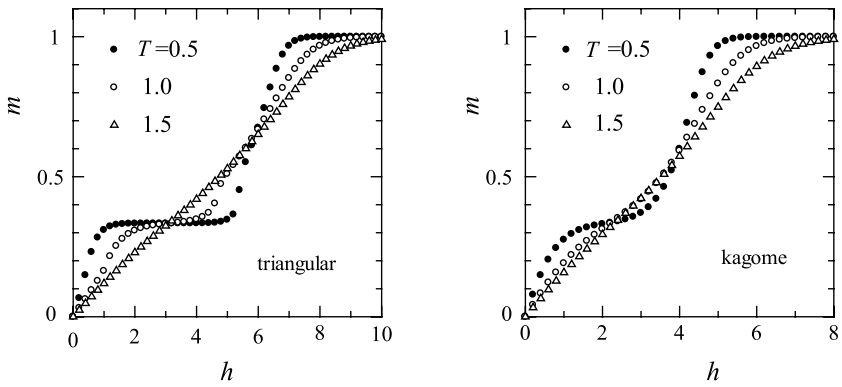

Figure 3. The magnetization per spin, m, as a function of h for three temperatures, in triangular and kagome lattices composed of $50 \times 50 \times 3$ spins by the MC method.

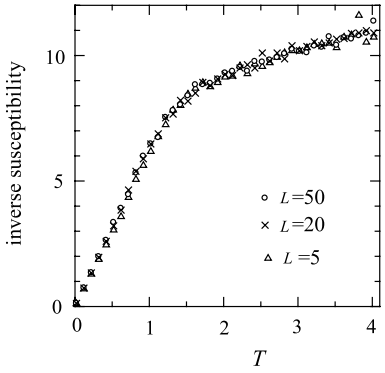

Figure 5. The system-size dependence of the inverse susceptibility per spin as a function of T for the triangular lattice. ○ represents $L = 50$, × represents $L = 20$ and △ represents $L = 5$.

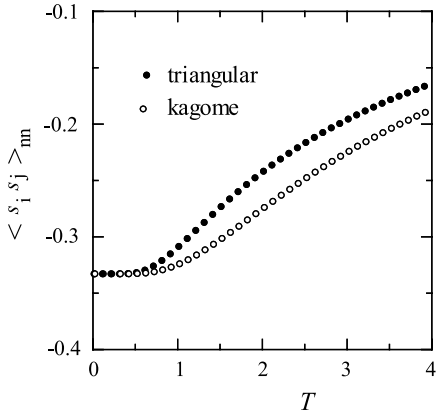

Figure 6. The nn spin correlation as a function of T for triangular and kagome lattices. The system size and the number of steps for MC averaging are the same as for the previous results.

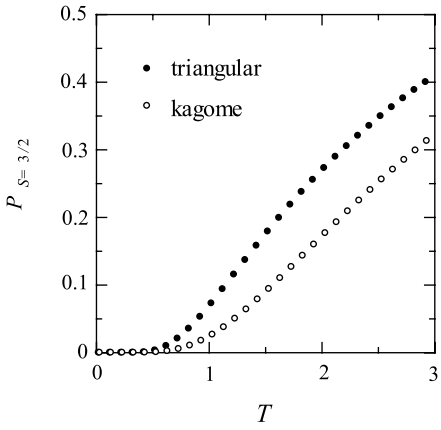

Figure 7. Probability $P_{S^z=3/2}$ of the number of excited quartet $S^z = 3/2$ triangles against the total number of triangles $2N_0$ as a function of T for triangular and kagome lattices.

studies have attributed this to the existence of 'orphan' or 'free' spins [16, 25]. However, it may not be conclusively decided whether the low-temperature Curie-like behavior comes from isolated free spins in a magnetically disordered or a quantum singlet background.

Free spins in triangular and kagome lattices may be produced, e.g. by introducing the three-sublattice structure: a site belonging to an A sublattice might be occupied by an up spin and its nn site belonging to an B sublattice by a down spin, then the third site belonging to the C sublattice may be 'free' as a central site of a hexagon forming the honeycomb lattice composed of A and B sublattices in the triangular lattice and as interpenetrating C sites between the stripes of the A–B-sublattice antiferromagnetic chains in the kagome lattice. In such a configuration, the number of free spins amounts to one-third the total number of spins. However, such an example with a symmetry breaking is only one of the degenerate ground states in the case of $h = 0$. Various states with other spin configurations may exist in the ground state manifold including one-third number of 'free' spins. Such an appearance of free spins is a feature of frustrated lattices.

For obtaining further insights, we investigated the temperature dependence of the nn correlation $\langle\sigma_i\sigma_j\rangle_{nn}$ and the probability $P_{S^z=3/2}$ of the number of excited $S^z = 3/2$ triangles among total number of triangles $2N_0$. These are shown in figures 6 and 7, respectively. The nn correlation at the lowest-temperature limit should take the value of $-1/3$ as easily recognized by considering the algebraic summation of nn bonds in any ground state configuration, because two spins are parallel but one is antiparallel in each triangle in the triangular and kagome lattices. As the temperature is increased above $T \sim 1$, nn spin correlation decreases in magnitude as shown in figure 6. This would be due to the excitation of a ferromagnetic bond against the antiferromagnetic interaction.

In addition, the probability of the existence of a triangle with three parallel spins, which we call the $S^z = 3/2$ triangle, $P_{S^z=3/2}$, is shown in figure 7. It begins to increase at $T \sim 1$ from zero with increasing temperature. In contrast, the two-up and one-down (or two-down and one-up) triangle, which we call the $S^z = 1/2$ triangle, decreases following $1 - P_{S^z=3/2}$, as has also been shown for the Ising model on garnet lattice [25].

The excitation of three-up (or three-down) $S^z = 3/2$ triangle well corresponds to the nn spin correlation for the change in the temperature dependence at $T \sim 1$ in figure 6.

The results in figures 6 and 7 support the idea that the total states in the ground state are constituted from the two-up and one-down (or one-up and two-down) triangles. Then, the mechanism of the anomalies in the thermodynamical properties shown above may be attributed to the excitation of a triangle plaquette from the $S^z = 1/2$ to the $S^z = 3/2$ triangle with increasing temperature. The picture of the triangle plaquette excitation might be consistent with the fact of the absence of system-size dependence of the gradient in Curie-like inverse susceptibility. The dominance of short-range correlation is well recognized as the general trend of geometrically frustrated lattices [26].

3. Exact calculation for single and small-size triangular clusters

Following the almost unremarkable system-size dependence of the thermodynamic properties shown in the previous section,

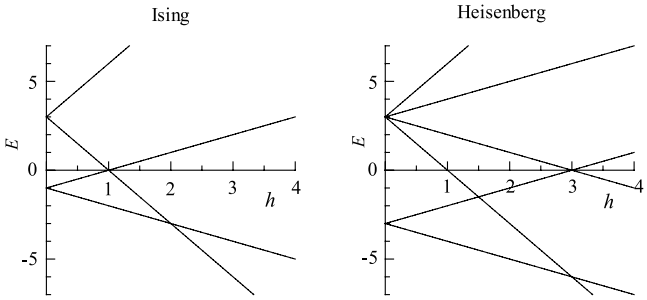

Figure 8. Energy spectra of Ising and Heisenberg models on a triangle cluster as a function of the magnetic field h.

Table 1. Eigenvalues and eigenfunctions of the Heisenberg model triangle cluster.

Eigenvalues	Eigenfunctions
$\varepsilon_1 = 3(1-h)$	$\|\phi_1\rangle$
$\varepsilon_2 = 3(1+h)$	$\|\phi_2\rangle$
$\varepsilon_3 = -(3+h)$	$\frac{1}{\sqrt{2}}(\|\phi_4\rangle - \|\phi_5\rangle)$
	$\frac{1}{\sqrt{6}}(-2\|\phi_3\rangle + \|\phi_4\rangle + \|\phi_5\rangle)$
$\varepsilon_4 = 3-h$	$\frac{1}{\sqrt{3}}(\|\phi_3\rangle + \|\phi_4\rangle + \|\phi_5\rangle)$
$\varepsilon_5 = -(3-h)$	$\frac{1}{\sqrt{2}}(\|\phi_7\rangle - \|\phi_8\rangle)$
	$\frac{1}{\sqrt{6}}(-2\|\phi_6\rangle + \|\phi_7\rangle + \|\phi_8\rangle)$
$\varepsilon_6 = 3+h$	$\frac{1}{\sqrt{3}}(\|\phi_6\rangle + \|\phi_7\rangle + \|\phi_8\rangle)$

we analytically executed the exact calculation for the three-spin equilateral triangle cluster. This was expected to reveal the dominance of short-range correlation on the intermediate temperature thermodynamical properties. In addition to the Ising model, the calculation was also done for the Heisenberg model.

We first consider the Ising single triangle cluster. For the system, the corresponding energies for $\tilde{H}$ in (1) are

$$E_1 = 3(1-h), \qquad E_2 = 3(1+h), \\ E_{3,4,5} = -(1+h), \qquad E_{6,7,8} = -(1-h), \tag{5}$$

for eight states of

$$|\phi_1\rangle = |\uparrow\uparrow\uparrow\rangle, \qquad |\phi_2\rangle = |\downarrow\downarrow\downarrow\rangle, \\ |\phi_3\rangle = |\uparrow\uparrow\downarrow\rangle, \qquad |\phi_4\rangle = |\uparrow\downarrow\uparrow\rangle, \\ |\phi_5\rangle = |\downarrow\uparrow\uparrow\rangle, \qquad |\phi_6\rangle = |\uparrow\downarrow\downarrow\rangle, \\ |\phi_7\rangle = |\downarrow\uparrow\downarrow\rangle, \qquad |\phi_8\rangle = |\downarrow\downarrow\uparrow\rangle, \tag{6}$$

where up and down arrows designate the respective spin of magnitude $1/2$. For a vanishing magnetic field $h = 0$, the ground state is the sixfold degenerate $S^z = 1/2$ states and the excited state is the twofold degenerate $S^z = 3/2$ states. Under the magnetic field, the degeneracy of the ground state is dissolved into two threefold degenerate states and that of the twofold degenerate excited state is lifted completely, as depicted in figure 8.

For the Heisenberg cluster, the Hamiltonian is given by adding the transverse component

$$\tilde{H}_t = 2J \sum_{\langle i,j \rangle} (s_i^+ s_j^- + s_i^- s_j^+), \tag{7}$$

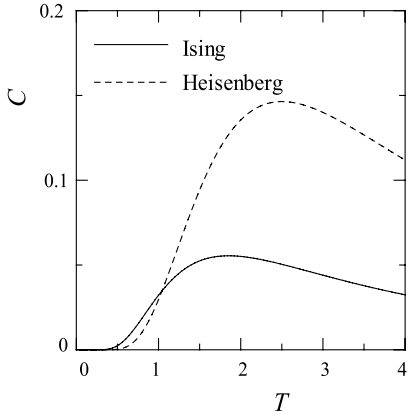

Figure 9. The specific heat per spin for a single triangle cluster as a function of T. Solid and broken curves denote data for the Ising and Heisenberg models, respectively.

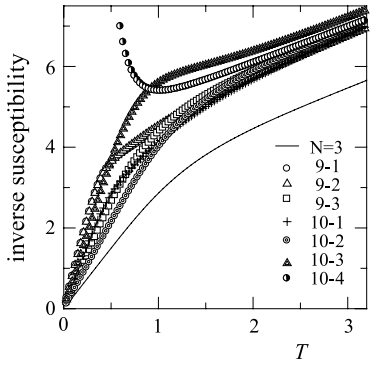

Figure 10. The inverse magnetic susceptibility per spin for Ising triangular clusters as a function of T. The solid line denotes that for a single triangle cluster, and those for three types of nine-site and four types of ten-site triangular clusters are denoted by 9-1, . . . , 9-3 and 10-1, . . . , 10-4, respectively. These finite clusters are depicted in figure 13. 10-4 denotes the curve for the ten-site two-leg truss-type cluster.

to (1). After the diagonalization procedure, the eigenvalues and eigenfunctions shown in table 1 and figure 8 were obtained.

For a vanishing field, the ground state is a fourfold degenerate doublet ($S = 1/2$) state with energy $\varepsilon_{3,5} = -3$ and the excited state is a fourfold degenerate quartet ($S = 3/2$) with $\varepsilon_{1,2,4,6} = 3$. The application of a magnetic field brings the ground state to the quartet state for $h > 3$ at $T = 0$ as shown in figure 8, resulting in metamagnetic behavior, as explicitly shown below.

The thermodynamic quantities such as specific heat, magnetic susceptibility and magnetization under a magnetic field can be calculated analytically by using the obtained energy spectra. The analytical expressions obtained are summarized in the appendix and are shown in figures 9–12. For these physical quantities, similar features emerge as for the MC simulation results for the triangular and kagome lattices, that is, the appearance of the hump in the specific heat, the downturn in the inverse susceptibility and the $1/3$ plateau in the magnetization process in the lower-temperature regime.

The hump in the specific heat data in figure 9 is found to be of Schottky type for both models, as recognized from the

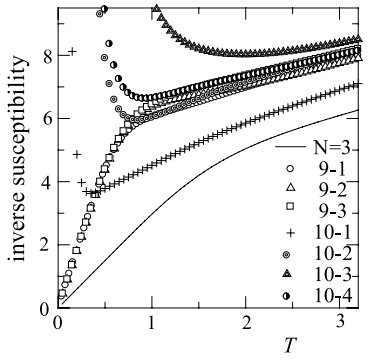

Figure 11. The inverse magnetic susceptibility per spin for Heisenberg triangular clusters as a function of T. The solid line denotes that for a single triangle cluster and those for three types of nine-site and four types of ten-site triangular clusters are denoted by 9-1, . . . , 9-3 and 10-1, . . . , 10-4, respectively.

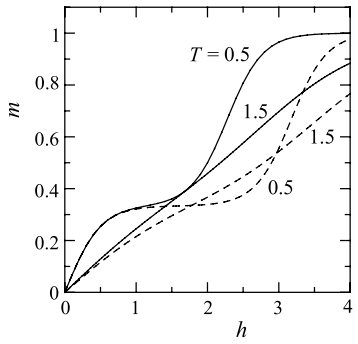

Figure 12. The magnetization per spin for a single triangle cluster as a function of h for $T = 0.5$ and 1.5, which are sufficiently lower than the characteristic temperatures and nearly equal to the characteristic temperatures, respectively. The solid and broken lines denote the data for the Ising and Heisenberg models, respectively.

two-level scheme in the energy spectra at $h = 0$ in (5) and table 1. It should be noted that the gap between the two levels is 4 and 6 for Ising and Heisenberg models, respectively, in units of J.

On the inverse susceptibility, the results for the Ising and Heisenberg models are shown by solid lines in figures 10 and 11, respectively. The low-temperature Curie-like behavior comes from the contribution of the ground S^z or $S = 1/2$ state for each respective model. By elevating the temperature, the excited S^z or $S = 3/2$ state begins to contribute near the characteristic temperature corresponding to the energy gap. The characteristic temperature corresponding to the hump of the specific heat and bending in the inverse susceptibility are denoted as $T_{\rm I}^{\rm c}$ and $T_{\rm H}^{\rm c}$ for the Ising and Heisenberg clusters, respectively. These temperatures have the same degree of magnitude as those for lattices, $T_{\rm triangular}^{\ell}$ and $T_{\rm kagome}^{\ell}$.

The magnetization under a magnetic field shows a 1/3 plateau, if the temperature is lower than $T_{\rm I}^{\rm c}$ or $T_{\rm H}^{\rm c}$ for each model, as shown in figure 12. The magnetic field and temperature dependence of magnetization are readily recognized from the energy spectra in figure 8. At a temperature of absolute zero, the magnetization at the limit of the weak field has a finite value of $m(T = 0, h \to 0) = 1/3$,

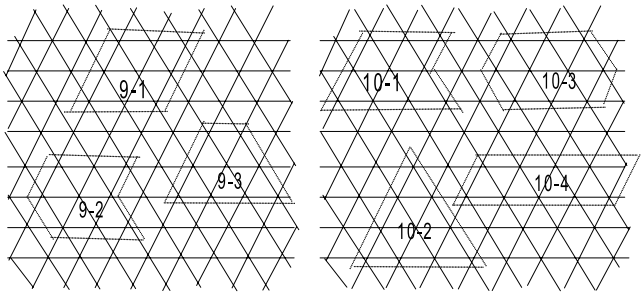

Figure 13. Finite triangular clusters used in exact-calculation studies of specific heat and inverse susceptibility. Depicted numbers correspond to those in figures 10 and 11.

in contrast to the case of the Ising-like anisotropic Heisenberg model [29]. The magnitude of h at the steep rise from the 1/3 plateau up to full polarization ($m = 1$) for sufficiently low temperature ($T \ll T_{\rm I,H}^{\rm c}$) is well accounted for from the ground state replacement due to the level crossing near $h = 2$ and 3 for the Ising and Heisenberg models, respectively, as is seen in figure 8. For temperatures higher than the characteristic temperature, these two levels are mixed thermally, and the plateau then disappears.

The qualitative consistency in these physical quantities between the single triangle cluster and for the MC results on two lattices suggest that the thermodynamical properties in the intermediate temperature regime at degree of J are dominated by the energy spectra of the triangle trimer. This agrees with the unrecognizable system-size dependence in the MC simulation results in the section 2.

To further substantiate the insight obtained, an exact numerical calculation of susceptibility and specific heat was carried out for several small-size clusters up to ten or 12 sites for triangular or kagome clusters, respectively, for the Ising model, and up to ten sites only for the triangular cluster for the Heisenberg model. The main features of the calculation are summarized as follows. In odd-spin-number clusters, the inverse susceptibility shows the downturn deviation without exception similar to the single triangle cluster case, irrespective of the geometry of kagome or triangular or spin models. However, for even-spin-number clusters, the results cannot be summarized so simply, because the cluster size could not be magnified for the Heisenberg model owing to limited availability of computational facilities. In the Ising case, the two-leg truss-type triangular clusters, like 10-4 in figure 13, show diverging deviation toward zero temperature from the Curie–Weiss-like high-temperature behavior, but all the other types of clusters investigated, such as one type for six sites, two types for eight sites and three types for ten sites in the triangular configuration and one type for 12 sites in the kagome configuration, show the downturn deviation as expected. On the other hand, for the Heisenberg model, the calculated four types of ten-site triangular clusters all show the diverging upturn in the inverse susceptibility. The doublet lowest-energy state of an odd number of sites was pointed out in kagome clusters [19]. Only some of the results of inverse susceptibility are shown in figures 10 and 11 for Ising and Heisenberg models, respectively, for triangular

clusters. Triangular clusters used in calculations are depicted in figure 13.

The specific heat has also been calculated for all of these clusters. In all cases, the hump at the temperature of order J has been recognized, although these are not shown in the figures.

We can thus conclusively state that for the Ising spin the triangle-based two-dimensional lattices are dominated by trimers in the intermediate-temperature regime, because an exceptional two-leg truss-type triangular structure should be regarded as pseudo-one-dimensional and not a two-dimensional triangle-based lattice. For the Heisenberg case, although the thermodynamical features cannot be attributed to trimer formation without showing the downturn behavior in even-site clusters with more extended magnitude, it is expected the behavior will be realized even in the Heisenberg model. The tendency of downturn is, for example, found in 10-1 and 10-2 clusters in figure 11, in a somewhat higher-temperature region than the temperature turning to the increase.

4. Conclusions and discussions

A mechanism for the downturn in inverse susceptibility exhibited by many two-dimensional triangle-based spin systems was proposed as an intrinsic property of triangle-based lattices, such as triangular and kagome lattices, by the simulation and exact calculation for single and small-size clusters of $s = 1/2$ Ising and Heisenberg models. Furthermore, it was found that near the temperature of bending in inverse susceptibility a hump in the specific heat appears, and below this temperature the $1/3$ magnetization plateau is revealed in its field dependence.

These thermodynamic features bear unremarkable system-size dependence in the MC simulations and were found even in a single triangle cluster, both in the Ising and the Heisenberg models. These results suggest the dominance of trimer formation. Additional exact numerical calculations for small-size clusters were carried out to confirm the expectations. For an Ising model, it is concluded that the intermediate-temperature properties of a two-dimensional triangle-based lattice are dominated by the trimer. On the other hand, for the Heisenberg model, conclusive results were not obtained by the calculation up to a ten-site cluster, although similar conclusions as for the Ising case are still expected by extended calculations to larger-sized clusters [18, 19, 34] with attention to the correlation between three quantities. The ground state is believed to be different for the triangular and the kagome lattices as an ordered and a singlet spin liquid state, respectively. Yet, the properties at intermediate temperature have not been clarified until now. The calculation for the extended-site clusters is desired for both triangular and kagome geometries. These are now in progress and will be reported in the future. Furthermore, we may speculate that this fact may safely interpret the similar temperature dependence found in three-dimensional triangle-based systems, such as garnet $Gd_3Ga_5O_{12}$ [9].

The specific heat hump and the bend in inverse susceptibility may be interpreted by the two-level energy scheme separated by a gap of the order of J (=1) of the trimer. The $1/3$ plateau under a magnetic field is due to the alignment of trimer spins below the characteristic temperature at negligibly weak fields ($h \ll 1$). For a finite weak field, the $1/3$ plateau may be realized by the three-sublattice configuration, where the A and B sublattices form the Néel state forming the honeycomb lattice and the C sublattice is free from nn interaction, for example, in the triangular lattice. Such a configuration at $h = 0$ is now known as the partial disordered state [22, 23], which does not stabilize as an ordered state [33].

Referring to real systems, $ZnCu_3(OH)_6Cl_2$, which has recently been studied as a prototype of the kagome system, shows the bending of the inverse susceptibility at about $T \sim 120$ K. The estimated coupling constant is $J \sim 17$ meV [8], corresponding well to the bending temperature. For SCGO, the bending is found at $T = 120$ K and $J \sim 100$ K [7]. The appearance of the hump of specific heat and of the $1/3$ plateau in magnetization is highly desired to be found at the corresponding temperature near $T/J \sim 1$. An example expected for the corresponding appearance of these three quantities may be in the triangle cluster compound $La_4Cu_3MoO_{12}$ [12]. Thus, in experimental studies, it is necessary to pay attention to the relationship between the three quantities discussed here, especially to the plateau, to which attention has not been paid previously.

Appendix

Analytical expressions for specific heat C, susceptibility χ and magnetization under magnetic field m of a single triangle cluster are summarized for the Ising and the Heisenberg models. These quantities are denoted with suffix I or H for the Ising or Heisenberg model, respectively.

The specific heat is given as

$$C_{\rm I} = \frac{1}{T^2}\left[\frac{1+3{\rm e}^{-4\beta}}{3+{\rm e}^{-4\beta}} - 3\left(\frac{1-{\rm e}^{-4\beta}}{3+{\rm e}^{-4\beta}}\right)^2\right],$$
$$C_{\rm H} = \frac{3}{T^2}\left[1-\left(\frac{1-{\rm e}^{-6\beta}}{1+{\rm e}^{-6\beta}}\right)^2\right], \tag{A.1}$$

and the susceptibility is

$$\chi_{\rm I} = \frac{1}{T}\frac{1+3{\rm e}^{-4\beta}}{3+{\rm e}^{-4\beta}},$$
$$\chi_{\rm H} = \frac{1}{3T}\frac{1+5{\rm e}^{-6\beta}}{1+{\rm e}^{-6\beta}}. \tag{A.2}$$

The magnetization under magnetic field h is expressed as

$$m_{\rm I} = \frac{h_{1-}^3 - h_{1+}^{-3} + h_{1+} - h_{1-}^{-1}}{h_{1-}^3 + h_{1+}^{-3} + 3(h_{1+} + h_{1-}^{-1})},$$
$$m_{\rm H} = \frac{1}{3}\frac{3(h_{1-}^3 - h_{1+}^{-3}) + 2(h_{3+} - h_{3-}^{-1}) + h_{3-} - h_{3+}^{-1}}{h_{1-}^3 + h_{1+}^{-3} + 2(h_{3+} + h_{3-}^{-1}) + h_{3-} + h_{3+}^{-1}}, \tag{A.3}$$

with $h_{p\pm} = \exp[\beta(h \pm p)]$.

References

[1] Diep H T 2004 *Frustrated Spin Systems* ed H T Diep (Singapore: World Scientific)
[2] Liebmann R 1986 *Statistical Mechanics of Periodic Frustrated Ising Systems* (Berlin: Springer)
[3] Ramirez A P 1994 *Annu. Rev. Mater. Sci.* **24** 453
[4] Schiffer P and Ramirez A P 1996 *Comment. Condens. Mater. Phys.* **18** 21
[5] Hirakawa K, Kadowaki H and Ubukoshi K 1985 *J. Phys. Soc. Japan* **54** 3526
[6] Ramirez A P, Espinosa G P and Cooper A S 1992 *Phys. Rev. Lett.* **64** 2070
Ramirez A P, Espinosa G P and Cooper A S 1992 *Phys. Rev.* B **45** 2505
[7] Schiffer P, Ramirez A P, Franklin K N and Cheong S-W 1996 *Phys. Rev. Lett.* **77** 2085
[8] Helton J S *et al* 2006 *Phys. Rev. Lett.* **98** 107204
[9] Schiffer P, Ramirez A P, Huse D A, Gammel P L, Yaron U, Bishop D J and Valentino A J 1995 *Phys. Rev. Lett.* **74** 2379
[10] Hiroi Z, Hanawa M, Kobayashi N, Nohara M, Takagi H, Kato Y and Takigawa M 2001 *J. Phys. Soc. Japan* **70** 3377
[11] Bono D, Mendels P, Collin G and Blanchard N 2004 *Phys. Rev. Lett.* **92** 217202
[12] Azuma M, Odaka T, Takano M, Vander Griend D A, Poeppelmeier K R, Narumi Y, Kindo K, Mizuno Y and Maekawa S 2000 *Phys. Rev.* B **62** R3588
[13] Robert J *et al* 2008 *Phys. Rev.* B **77** 054421
[14] Sano K 1987 *Prog. Theor. Phys.* **77** 287
[15] Moessner R and Berlinsky A J 1999 *Phys. Rev. Lett.* **83** 3293
[16] Schiffer P and Daruka I 1997 *Phys. Rev.* B **56** 13712
[17] Zheng W, Singh R R P, Mckenzie R H and Coldea R 2005 *Phys. Rev.* B **71** 134422
[18] Elstner N, Singh R R P and Young A P 1993 *Phys. Rev. Lett.* **71** 1629
[19] Elstner N and Young A P 1994 *Phys. Rev.* B **50** 6871
[20] Rigol M and Singh R R P 2007 *Phys. Rev.* B **76** 184403
[21] Bert F, Nakamae S, Ladieu F, L'Hôte D, Bonville P, Duc F, Trombe J-C and Mendels P 2007 *Phys. Rev.* B **76** 132411
[22] Takagi T and Mekata M 1995 *J. Phys. Soc. Japan* **64** 4609
[23] Takagi T and Mekata M 1993 *J. Phys. Soc. Japan* **62** 3943
[24] Wada K and Ishikawa T 1983 *J. Phys. Soc. Japan* **52** 1774
[25] Yoshioka T, Koga A and Kawakami N 2004 *J. Phys. Soc. Japan* **73** 1805
[26] Moessner R and Chalker J T 1998 *Phys. Rev.* B **58** 12049
[27] Metcalf B D 1973 *Phys. Lett.* A **45** 1
[28] Miyashita S 1986 *J. Phys. Soc. Japan* **55** 3605
[29] Nishimori H and Miyashita S 1986 *J. Phys. Soc. Japan* **55** 4448
[30] Honecker A, Schulenburg J and Richter J 2004 *J. Phys.: Condens. Matter* **16** S749
[31] Zhitomirsky M E 2002 *Phys. Rev. Lett.* **88** 057204
[32] Hida K 2001 *J. Phys. Soc. Japan* **70** 3673
[33] Wada K, Tsukada T and Ishikawa T 1982 *J. Phys. Soc. Japan* **51** 1331
[34] Misguich G and Sindzingre P 2007 *Eur. Phys. J.* B **59** 305